

A handwriting method for low-cost gas sensors

*F. Loghin*¹, *A. Falco*², *A. Albrecht*¹, *J. Salmerón*¹, *M. Becherer*¹, *P. Lugli*², *A. Rivandeneira*¹

¹Institute for Nanoelectronics, Technische Universität München, Munich, Germany

²Faculty of Science and Technology, Free University of Bozen-Bolzano, Bozen-Bolzano, Italy

KEYWORDS. Ball pen, carbon nanotubes, flexible substrate, relative humidity, resistive sensor, silver nanoparticles

ABSTRACT

In this study, we report on an automated method based on a handwritten technique for the fabrication of low-cost gas sensors based on carbon nanotube (CNT) networks. Taking advantage of the inherent low-cost, flexible and uncomplicated characteristics of pen based techniques and combining them with an automated robotic system allows for high-resolution patterns, high reproducibility and relatively high throughput considering the limitations of parallel processing. To showcase this, gas sensors capable of sensing NH₃, CO₂, CO and Ethanol as well as temperature and relative humidity are fabricated and characterized displaying competitive performance in relation to previously reported devices. The presented process is compatible with a variety of solutions and inks, and, as such, allowing for an easy integration

1
2
3 into existing printing and coating frameworks with the greatest advantage being the ease of
4 creating prototypes due to the non-stringent material requirements.
5
6
7
8
9
10

11 INTRODUCTION

12
13
14

15 The concept of the Internet of Things (IoT) has opened a new paradigm in the interaction
16 between objects and human beings. In the IoT, sensors and actuators are embedded in physical
17 objects and interconnected through wired and wireless networks, creating new opportunities for
18 hardware, software and applications. In this regard, sensors play a fundamental role in extracting
19 valuable information regarding the object and its environment ¹. There have been many advances
20 in the development of sensors with emerging technologies. In particular, flexible and printed
21 electronics are catching the attraction of new sensors developments thanks to the versatility that
22 they offer in terms of new and outstanding features and, therefore, ground-breaking
23 applications². Among these new characteristics are biodegradable materials, large-scale and low-
24 cost processes and self-designed circuits ³. The most common used manufacturing techniques in
25 this area are inkjet printing and screen printing. The former controls the amount of material
26 deposited with virtually no wastes while defining the pattern and avoids the contact between the
27 substrate and the inkjet head ⁴. Whereas the latter technology provides a fast fabrication process
28 with thicker layers although wastes are unavoidable ⁵. Although both techniques reduce costs
29 compared to silicon based technology as no clean room, high temperature or vacuum processes
30 are involved, in addition to new materials and fabrication steps being easily integrable, the
31 prototyping costs are still high. There are some examples in the literature where a normal inkjet
32 printer has been used to manufacture circuits ⁶. In this regard, a new trend, known as handwriting
33
34
35
36
37
38
39
40
41
42
43
44
45
46
47
48
49
50
51
52
53
54
55
56
57
58
59
60

1
2
3 electronics, is catching the attention to fill these gaps ⁷. On one hand, commercial pencils have
4 been already employed to define the anode and cathode of paper based fuel cells ⁸ and the
5 resistor element of filters ⁹. There are also advances in the direction of process-enhanced
6 nanocarbon for integrated logic (PENCILs), broadening the possibilities of conventional
7 graphite-based pencils. PENCILs uses solid composites fabricated by mechanical mixing and
8 subsequent compression into a form similar to a conventional pencil “lead” and these solid
9 composites are then deposited by mechanical abrasion (“drawing”) on the surface of paper to
10 generate functional devices ¹⁰. However, this method is limited in throughput, precision, and
11 surface compatibility for interconnects. The inclusion of a posterior step after PENCILs, known
12 as deposition of resistor with abrasion fabrication technique (DRAFT), enhances the obtained
13 throughput, precision, and surface compatibility ¹¹. On the other hand, fountain pens and ball
14 pens have been used to fabricate electronics by substituting their colour ink by functionalized
15 ones. For example, a light emitting diode (LED) circuit, a chemical sensor ¹² and biocatalytic
16 sensor for home-based low-cost diabetes diagnosis have been reported using these strategies ¹³.

17
18
19
20
21
22
23
24
25
26
27
28
29
30
31
32
33
34
35
36 With respect to sensors, new materials such as semiconducting metal oxides ¹⁴, graphene oxide
37 ¹⁵, organic materials ¹⁶, and carbon black–polymer composites ¹⁷, have caught lot of attention
38 towards overcoming the drawbacks of conventional gas sensing techniques (i.e. gas
39 chromatography (GC), also coupled to mass spectrometry or atomic emission detection) ¹⁸. One recently
40 quite used material for gas sensors are carbon nanotubes (CNTs). The majority of these CNT-
41 based gas sensors employed more sophisticated techniques, such as sputtering or chemical vapor
42 deposition (CVD), to define this sensing layer, requiring very specific manufacturing conditions
43 and, therefore, resulting in high cost devices ¹⁹. Other commonly used techniques are coating
44 techniques such as drop-casting or spin-coating, limiting the resolution and possibilities of the
45
46
47
48
49
50
51
52
53
54
55
56
57
58
59
60

1
2
3 sensors²⁰. Furthermore, there are very few examples where the same fabrication technique is
4 used for both electrodes and sensing layer, so that the compatibility among processes plays a
5 larger role thus increasing the final device cost and feasibility¹¹. Our solution compromises non-
6 special conditions to manufacture, while guaranteeing a high degree of resolution and reliability,
7 employing the same fabrication process for all the layers involved.
8
9

10
11 In terms of performance, the sensors, which show a relative selective response to other
12 chemical species, possess a functionalized sensing layer^{20c, 21}. Those based only on CNT as the
13 sensor described in this paper exhibit a poor behavior in terms of selectivity^{19a, 22}. Although this
14 is not the purpose of this paper, the selectivity could be enhanced by functionalization of the
15 CNT ink by the addition of metal nanoparticles as shown in²³. The only requirement of this
16 strategy is that the viscosity of the custom-made ink remains below 10 cp.
17
18
19
20
21
22
23
24
25
26
27

28
29 In this paper we demonstrate how easily an electronic prototype can be realized in a
30 reproducible way by using a ball pen in terms of layout and nominal resistance. In order to
31 provide this reproducibility, the fabrication process is automated through an arm-robot. We
32 designed a resistive gas sensor using this technique. The sensor is drawn on poster foil substrate
33 whose sensing layer is made of CNTs. Previous works have demonstrated the efficiency of this
34 layer for sensing purposes²⁴, how it can be defined by printing methods²⁵ and how the sensors
35 can be reset in simple and energy-efficient ways²⁶. Here, we show how inks with varying
36 solvents and material loads can be employed with a commercial ball-pen to define accurate
37 electronic circuits with a performance comparable to higher cost technologies. Such a solution
38 provides a fast prototyping tool and opens the electronics to the so-called do-it-yourself (DIY)
39 paradigm, providing high resolution and versatility to produce cost-effective sensors.
40
41
42
43
44
45
46
47
48
49
50
51
52
53
54
55
56
57
58
59
60

MATERIALS AND METHODS

Device Fabrication

The devices presented in this manuscript were fabricated with the aid of a ballpoint pen with a sphere diameter of 0.7 mm. The pen and cartridge (Schmidt Technology) are fixated in a 2-stage plotter (x-y axis) with variable height adjustment (z-axis). No extra weight was added and contact force between the pen and substrate consists of the pen's, ink's and holder's weight. Figure 1a displays the writing setup with the pen in contact with the substrate. The movement speed was set at 25 mm/s. As a substrate, untreated grayback polypropylene (PP) poster foil (EMBLEM) was used. The writing process was performed in ambient lab conditions with no additional heating. For the definition of the contacts, a silver nanoparticle ink (AgNP) (Sigma-Aldrich) with a load of 30-35 wt% with a maximum particle size of 50 nm was used. The ink solvent was triethylene glycol monomethyl ether (TGME). In order to reduce the resistance of the contacts the hatching was performed both at 90° and 180° angle. This also reduces the chance of defects as well as any artefacts, which are writing direction dependent. The samples were photonicallly sintered (Xenon) with a pulse width of 500 μ s and a periodicity of 1s 15 times following the optimization described in a previous work for the same silver ink²⁷. The active area (Figure 1b) was written subsequently using a custom-made CNT ink²⁸ with one pass over. The ink consists of 0.03 wt% CNT (Carbon Solution INC) dispersed with the aid of sodium dodecyl sulphate (SDS) in deionized water (DI H₂O). The sample was submerged in DI H₂O for 10 min to remove the SDS as this acts as a weak insulator as well as shielding the CNTs from the analyte.

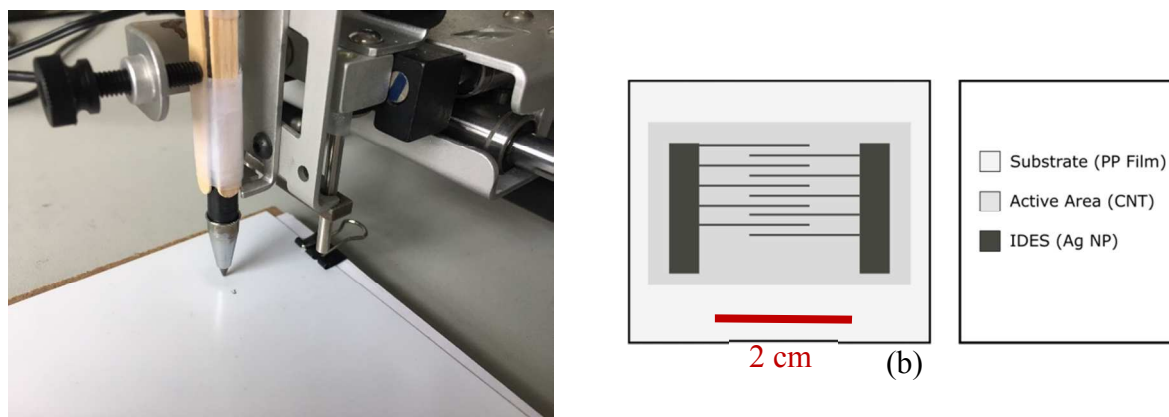


Figure 1. (a) Photograph of ball pen in the robot arm employed to develop the printed sensor (b) Schematic of the sensor depicting critical layers.

Device Characterization

For the CNT film and AgNP electrode morphology characterization, scanning electron microscopy (SEM) was performed. SEM-images were recorded with a field-emission scanning electron microscope (NVision40 from Carl Zeiss) at an extraction and acceleration voltage of 5 and 7 kV, respectively. To optimize the image quality, the working distance was adjusted in the range 5-6 mm.

For the gas measurements, the sample (Figure 2a) was fixed onto a module consisting of a Peltier-heating element used for temperature control, a Pt100 for in-situ temperature monitoring and leads for contacting the sensor (Figure 2b). The holder was inserted into a self-made gas chamber into which gasses can be fluxed (see Figure S2). The sensor response to ammonia (NH_3), ethanol (Eth) and carbon monoxide (CO) was characterized by exposing the sample to various concentrations of the test gas. In order to maintain a constant flux, a carrier gas (N_2) was mixed with NH_3 , Eth or CO to generate different concentrations. In an analogue manner, carbon dioxide (CO_2) was mixed with pressurized air to regulate the concentration. A standard

1
2
3 measurement cycle consists of an active recovery cycle at 60 °C for 300 s to recover the sensor
4 to its original state followed by a 300 s exposure cycle where the test concentration was fluxed.
5
6
7
8 The total flux was kept constant to 200 ml/min. The measurement was automated with the use of
9
10 LabVIEW 2016, which controls a source meter (Keithley 2602A) for the Pt100 and Peltier
11
12 element, as well as an impedance analyzer (Keysight E4990A) with an impedance probe kit
13
14 (4294A1) for the sensor readout. The excitation voltage applied in all measurements was $V_{DC} = 0$
15
16 and $V_{AC} = 500$ mV and the frequency was 20 Hz.
17
18
19

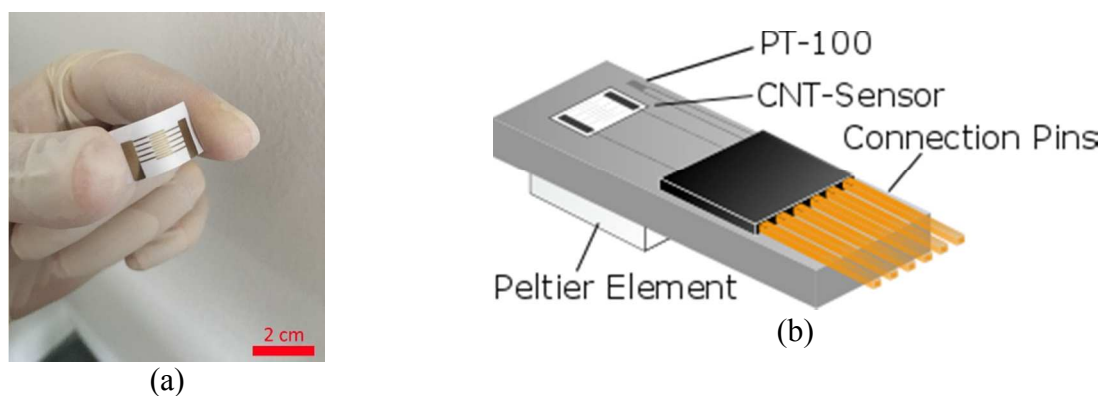


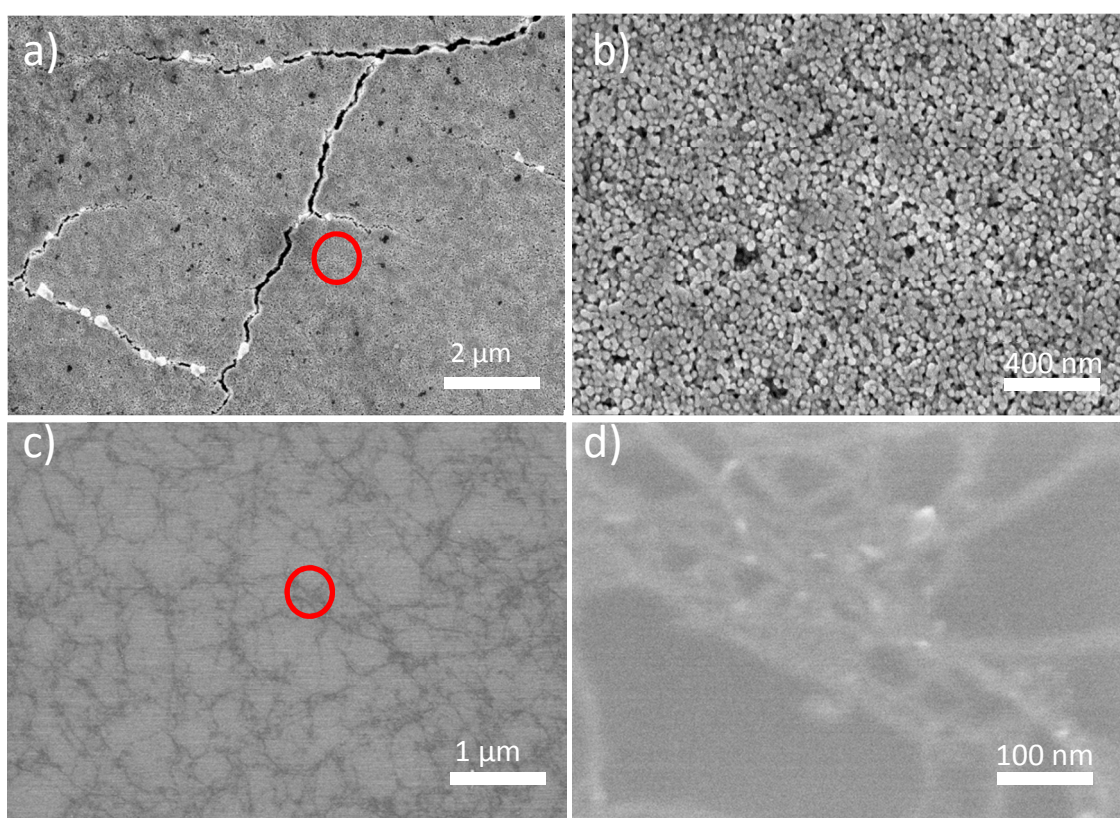
Figure 2. (a) Photograph of the fabricated sensor; (b) schematic depicting the sensor module

The above-mentioned module was placed in a climatic chamber (VLC4006) with the temperature/humidity control. Monitoring was performed over the climatic chamber sensor system. For the humidity sensing the humidity was ramped up in 15% steps and held for 600 s. A similar approach was used for the temperature sensing with 5 °C steps for 300 s. The chamber was filled with ambient air and no conscious effort was made to regulate this.

RESULTS

The characterization of the deposited films was performed by SEM for a better understanding of the resulting films. From the resulting images of the AgNP films, (Figure 3 (a-b)) a homogeneous film can be observed especially at the 25kx magnification. Visible is the typical

1
2
3 necking of the AgNPs that is characteristic to sintered AgNP films²⁷. At lower magnification
4 (5kx) microcracks can be observed. Although the precise origin of these cracks needs to be
5 investigated, in the current device architecture, due to the large difference in contribution to the
6 device resistance between contacts and active film, it can be neglected. The CNT films exhibit
7 (Figure 3 (c-d)) a good distribution of CNT across the substrate with a good debundling visible
8 at higher magnification (200kx).



9
10
11
12
13
14
15
16
17
18
19
20
21
22
23
24
25
26
27
28
29
30
31
32
33
34
35
36
37
38
39
40
41
42
43
44
45
46
47
48
49
50
51
52
53
54
55
56
57
58
59
60

Figure 3. (a-b) Scanning electron microscope image of the silver nanoparticle film at (a) 5K (1 μm scale) and (b) 25 K (200 nm scale bar) magnification with the red circle depicting the higher magnification region. (c-d)) Scanning electron microscope image of the CNT film at (a) 20K (1 μm scale) and (b) 200K (100 nm scale bar) magnification with the red circle depicting the higher magnification region.

1
2
3 A set of 20 sensors was written with a nominal value of resistance measure at ambient conditions
4 of $1.6 \pm 0.3 \text{ k}\Omega$. In all cases the phase of the devices was below $-5 \cdot 10^{-4}^\circ$, indicating the pure
5 resistive behaviour of our sensors.
6
7

8
9
10 The sensor performance was evaluated by its normalized response, defined in (1) as the relative
11 change in resistance with respect to its initial value,
12
13

$$14 \quad \text{Norm. Resistance (\%)} = \frac{R_f - R_i}{R_i} \cdot 100 \quad (1)$$

15
16
17
18
19
20 where R_i and R_f are the initial and final resistance values of an exposure cycle, respectively.

21
22 Figure 4 illustrates the characterization of the sensor towards NH_3 . Higher temperatures were not
23 considered to avoid the degradation of the substrate. Figure 4a shows the calibration curve of the
24 sensor for NH_3 .
25
26
27
28
29

30
31 In comparison with other printed gas sensors based on CNTs as sensing material, the response of
32 the developed sensors is consistent. In the cases of the studied gases, the resistance of the sensor
33 increases when it is exposed to any of them. The same trend is observed when the sensor is under
34 increasing content of moisture. In contrast to this, the resistance value decreases when the sensor
35 is analysed with increases in temperature ²⁹.
36
37
38
39
40
41
42
43
44
45
46
47
48
49
50
51
52
53
54
55
56
57
58
59
60

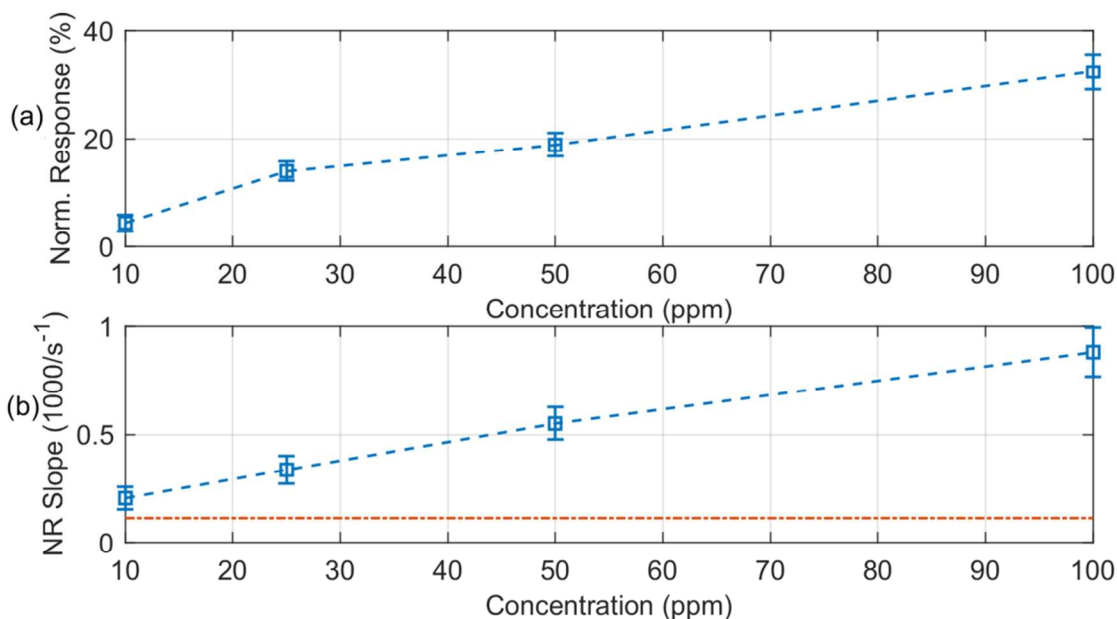


Figure 4. Response to NH_3 (a) Normalized resistance vs. concentration; (b) Average slope of the normalized response in the first 150 s of exposure. The red dashed line indicates the average slope of the normalized response in the last 150 s of cooling time.

In particular, the response to NH_3 is much higher than the change obtained towards the other gases. For example, the normalized variation in resistance at 50 ppm of ammonia is about 20%, whereas the change at 50 ppm ethanol is about 7% (Figure 5c) and this variation is about 4.5% for CO (Figure 5b). In the case of CO_2 , the measured concentrations are much higher because the normal air used as carrier gas typically contains 390 ppm of CO_2 , which is the reason for the high concentration range covered in our tests (Figure 5a).

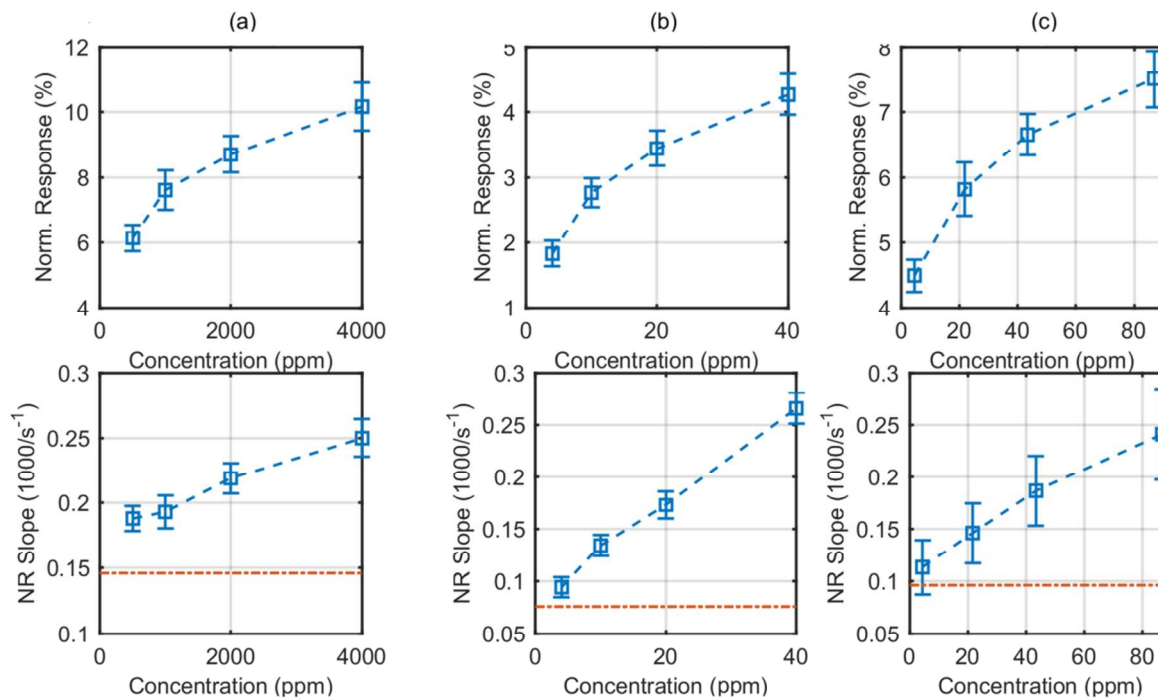


Figure 5. First row corresponds to the normalized resistance, bottom row to average slope of the normalized response in the first 150 s of exposure vs. concentration for (a) CO₂, (b) CO and (c) Ethanol. In the bottom row the red dashed line indicates the average slope of the normalized response in the last 150 s of cooling time.

With respect to the response of the sensor to moisture content (Figure 6a), the variation in resistance also shows a direct increase with the humidity level, with a variation above 30% at 90%RH. Looking at the behaviour with temperature (Figure 6b), the resistance decreases with the increase in temperature, as expected because temperature facilitates the carriers to cross the barriers at the junctions. Notice that the ambient conditions were set at 25% RH and 25 °C.

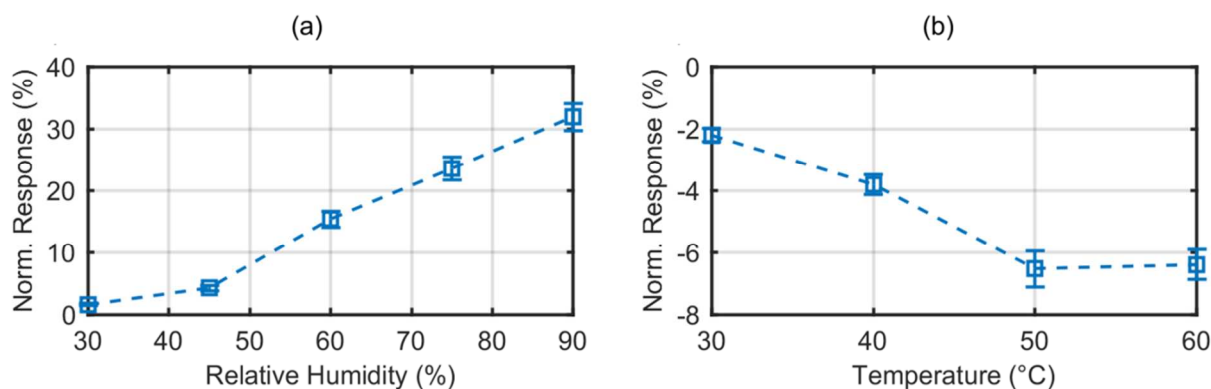


Figure 6. Normalized resistance vs. concentration for (a) RH and (b) Temperature.

Table 1 summarizes the performance of the device with respect to each parameter studied to facilitate comparison.

Table 1. Summary of the main features of developed sensor response. NR stands for Normalized resistance

Parameter	Range	Sensitivity	Recovery (°C)	Exposure Time (s)	Linearity (R^2)
NH ₃	10-100 ppm	0.3 %NR/ppm	60 (300 s)	300	0.9642
CO	5-45 ppm	0.06 %NR/ppm	60 (300 s)	300	0.9169
Ethanol	5-80 ppm	0.03 %NR/ppm	60 (300 s)	300	0.8996
CO ₂	500-4000 ppm	0.011 %NR/ppm	60 (300 s)	300	0.9182
RH	30-90%	0.5 %NR/%RH	60 (600 s)	600	0.9768
Temperature	30-65 °C	-0.217 %NR/°C 30<T<50 °C No sensitivity T>50 °C	--	600	0.9775

DISCUSSION

1
2
3 Our sensor shows a 5%NR at 10 ppm and 20%NR at 50 ppm NH₃ values very similar to
4 previous developed devices (see Table 2). Nevertheless, the advantages of our approach provides
5 high value to our sensor: the CNT layer did not required any functionalization, the fabrication
6 process is low-cost using the same procedure to define all the layers and it is done at room
7 conditions without special requirements. Furthermore, the sensor is defined on a flexible and
8 biodegradable substrate, resulting in conformally-shaped devices and reducing wastes.
9

10
11
12 In the case of CO₂, as commented before, we could not test the sensor at lower concentrations
13 due to constrains in the setup. However, our sensor exhibits almost 8%NR at 1000 ppm, which is
14 very similar to the response of Lin et al. 2016³⁰. With respect to CO, we tested very low
15 concentrations in comparison with other CO sensors based on CNTs and our device presents a
16 higher response than those examples (see Table 2). For moisture content, the sensor described in
17 this work shows about 18%NR at 60%RH and about 32%NR at 90%RH. Again, this response is
18 comparable to previous works, proving that this technique offers the same performance as
19 sophisticated fabrication methods.
20
21
22
23
24
25
26
27
28
29
30
31
32
33
34

35 It must be highlighted the fact that the majority of the authors do not study the response of
36 their devices with respect to other gas species or environmental parameters, and therefore, the
37 selectivity or the behavior of the sensor under real working conditions is not tested as illustrated
38 in this work. It is clear that our device requires some kind of functionalization or treatment to
39 achieve a better selectivity but it has been already proved that the decoration of CNTs with metal
40 nanoparticles enhanced the selectivity of CNT-based gas sensors^{23, 31}. Furthermore, the use of
41 sensor arrays for multicomponent analysis using multivariate calibration software can achieve
42 improved analyte sensitivity.
43
44
45
46
47
48
49
50
51
52
53

54 **Table 2.** Summary of developed gas sensors based on CNTs. All the sensors are resistive.
55
56
57
58
59
60

Reference	Fabrication method	Sensing layer	Gas	Sensitivity	Range
Schütt et al 2017 ^{19b}	Glass substrate, patterned contacts	Single and Networked ZnO–CNT	NH ₃	6.4 NR%/ppm	10-100 ppm
Hester et al. 2015 ^{22a}	Kapton substrate, Graphene oxide electrodes inkjet printing	single wall CNTs (SWCNTs)	NH ₃	2.8 %NR at 10 ppm	10 ppm
Mirica et al. 2012 ¹¹	Handwriting DRAWN	CNT and graphite	NH ₃	1.8%NR at 10 ppm	1-10 ppm
Eising et al. 2017 ^{21a}	Silicon substrate, sputtering electrodes	PANI: multi wall CNTs (MWCNTs) films	NH ₃	40%NR at 30 ppm	30-60 ppm
This work	Pen ball	SWCNT	NH ₃	20%NR at 50 ppm	10-100 ppm
Ellis et al. 2016 ^{21b}	Silicon substrate, drop casting	In ₂ O ₃ /SWCNT	Ethanol	0.1285%NR/ppm log. Response	1-100 ppm
Zhang et al. 2014 ³²	layer-by-layer self-assembly	(MWCNTs)/polymer	Ethanol	4%NR at 30kppm	1 kppm – 30k ppm
This work	Pen ball	SWCNT	Ethanol	6%NR at 20 ppm	5-80 ppm
Liu et al. 2016 ^{20a}	Drop-casting on glass evaporated electrodes	organocobalt complex and SWCNT	CO	1.2%NR at 3kppm	800-6000 ppm
Hannon et al. 2014 ^{22b}	Silicon wafer	SWCNT	CO	0.0023%NR/ppm Exp. Response	1-60 ppm
This work	Pen ball	SWCNT	CO	3.5%NR at 20 ppm	5-45 ppm
Young et al. 2017 ^{19a}	CNTs grown by CVD transferred to a flexible one	CNT	CO ₂	1%NR at 50 ppm	50-800 ppm
Lin et al. 2016 ³⁰	CNTs grown by CVD transferred to a flexible one	Au coated MWCNTs	CO ₂ NH ₃	4.8%NR at 800 ppm CO ₂ 5.2%NR at 800 ppm NH ₃	50-800 ppm

This work	Pen ball	SWCNT	CO ₂	8%NR at 1000 ppm	500-4000 ppm
Jung et al. 2014 ^{20b}	spin-coating	MWCNTs	RH	60%NR at 60%RH	10-90%
Jung et al. 2015 ^{20c}	spin-coating	CNT/MnO ₂	RH	60%NR at 90%RH	10-90%
Zhao et al. 2017 ³³	Commercial pencil and ink marker	Oxidized MWCNT	RH	18-33% ($\Delta I/I_0$)	33-90%RH
This work	Pen ball	SWCNT	RH	20%NR at 60%RH	30-90%RH
Honda et al. 2014 ³⁴	Shadow mask printing on kapton	PEDOT:PSS and CNTs	Temperature	0.6 %NR/ °C	20-50 °C
This work	Pen ball	SWCNT	Temperature	-4%NR at 40 °C	30-65 °C

Finally, in order to assess the long-term stability of the sensor, we performed an analysis of the sensitivity comparing the normalized response one day after fabrication and one year after fabrication. The sensors were kept in a kitchen room, exposed to air, light and all the environmental agents, which would interact with them during their normal employment as air-quality sensors. Figure 7 shows how, besides the lowest part of the normalized response curve, the evaluated response after one year is very consistent with freshly fabricated sensors.

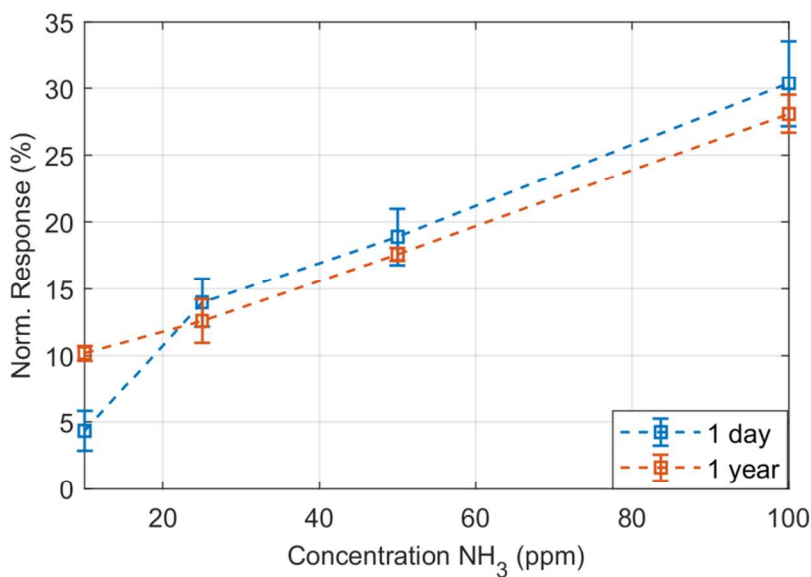


Figure 7. Normalized response with respect to different concentrations of NH₃ for the same sensor one day after fabrication (blue line) and one year after fabrication (orange line).

CONCLUSIONS

In this paper, we introduced a low cost fabrication technique based on a hand writing method (ballpoint pen) which allows for fast prototyping as well as do-it yourself electronics. In particular, we extended the inherent advantages of the existing technique by incorporating it into an automated robotic system that allows for high-resolution patterns, high reproducibility and relatively high throughput considering the limitations of parallel processing. Such characteristics had not previously been achieved with handwritten electronics. The process here highlighted is compatible with both commercial and custom-made inks providing versatile and flexible manufacturing, allowing for the incorporation into existing printing and coating frameworks. As a proof of concept, a sensing element was developed able to detect NH₃, CO₂, CO and Ethanol in a controlled environment, delivering comparable results to previously reported devices realized

1
2
3 with significantly more sophisticated techniques. The sensor was also characterized with respect
4
5 to relative humidity as well as temperature to account for cross sensitivity to changing
6
7 environmental conditions.
8
9

11 AUTHOR INFORMATION

15 **Corresponding Author**

16
17 Dr.-Ing. Almudena Rivadeneyra

18
19
20 Institute for Nanoelectronics, Technische Universität München

21
22
23 Theresienstrasse 90, 80333 Munich, Germany

24
25
26
27 Email: almudena.rivadeneyra@tum.de
28
29

31 **Author Contributions**

32
33 The manuscript was written through contributions of all authors. All authors have given approval
34
35 to the final version of the manuscript.
36
37
38
39
40
41

42 ACKNOWLEDGMENT

43
44
45 This work was partially funded by the TUM Graduate School.
46
47
48
49

50 REFERENCES

- 51
52
53 1. Chui, M.; Löffler, M.; Roberts, R., The Internet of Things. *McKinsey Quarterly* **2010**, *2*
54
55 (2010), 1-9.
56
57
58
59
60

1
2
3 2. (a) Fernández-Salmerón, J.; Rivadeneyra, A.; Martínez-Martí, F.; Capitán-Vallvey, L. F.;
4 Palma, A. J.; Carvajal, M. A., Passive UHF RFID Tag with Multiple Sensing Capabilities.
5
6 *Sensors* **2015**, *15* (10), 26769-26782; (b) Mattana, G.; Briand, D., Recent Advances in Printed
7
8 Sensors On Foil. *Materials Today* **2016**, *19* (2), 88-99; (c) Rivadeneyra, A.; Fernández-
9
10 Salmerón, J.; Agudo-Acemel, M.; López-Villanueva, J. A.; Capitan-Vallvey, L. F.; Palma, A. J.,
11
12 Printed Electrodes Structures As Capacitive Humidity Sensors: A Comparison. *Sensors and*
13
14 *Actuators A: Physical* **2016**, *244*, 56-65; (d) Alkin, K.; Stockinger, T.; Zirkl, M.; Stadlober, B.;
15
16 Bauer-Gogonea, S.; Kaltenbrunner, M.; Bauer, S.; Müller, U.; Schwödiauer, R., Paper-based
17
18 Printed Impedance Sensors for Water Sorption And Humidity Analysis. *Flexible and Printed*
19
20 *Electronics* **2017**, *2* (1), 014005.
21
22
23
24
25

26
27 3. Suganuma, K., *Introduction to printed electronics*. Springer Science & Business Media:
28
29 2014; Vol. 74.
30
31

32
33 4. Calvert, P., Inkjet printing For Materials and Devices. *Chemistry of Materials* **2001**, *13*
34
35 (10), 3299-3305.
36
37

38
39 5. Parashkov, R.; Becker, E.; Riedl, T.; Johannes, H.-H.; Kowalsky, W., Large Area
40
41 Electronics Using Printing Methods. *Proceedings of the IEEE* **2005**, *93* (7), 1321-1329.
42

43
44 6. (a) Lee, H.-H.; Chou, K.-S.; Huang, K.-C., Inkjet printing of nanosized silver colloids.
45
46 *Nanotechnology* **2005**, *16* (10), 2436; (b) Kawahara, Y.; Hodges, S.; Cook, B. S.; Zhang, C.;
47
48 Abowd, G. D. In *Instant inkjet circuits: lab-based inkjet printing to support rapid prototyping of*
49
50 *UbiComp devices*, Proceedings of the 2013 ACM international joint conference on Pervasive and
51
52 ubiquitous computing, ACM: 2013; pp 363-372; (c) Tortorich, R. P.; Choi, J.-W., Inkjet printing
53
54 of carbon nanotubes. *Nanomaterials* **2013**, *3* (3), 453-468.
55
56
57
58
59
60

- 1
2
3 7. Li, Z.; Liu, H.; Ouyang, C.; Hong Wee, W.; Cui, X.; Jian Lu, T.; Pingguan□Murphy, B.;
4
5 Li, F.; Xu, F., Recent Advances in Pen□Based Writing Electronics and their Emerging
6
7 Applications. *Advanced Functional Materials* **2016**, *26* (2), 165-180.
8
9
- 10 8. Dossi, N.; Toniolo, R.; Piccin, E.; Susmel, S.; Pizzariello, A.; Bontempelli, G., Pencil□
11
12 Drawn Dual Electrode Detectors to Discriminate Between Analytes Comigrating on Paper□
13
14 Based Fluidic Devices but Undergoing Electrochemical Processes with Different Reversibility.
15
16 *Electroanalysis* **2013**, *25* (11), 2515-2522.
17
18
- 19 9. Kurra, N.; Dutta, D.; Kulkarni, G. U., Field Effect Transistors and RC Filters from
20
21 Pencil-trace on Paper. *Physical Chemistry Chemical Physics* **2013**, *15* (21), 8367-8372.
22
23
24
25
- 26 10. (a) Mirica, K. A.; Azzarelli, J. M.; Weis, J. G.; Schnorr, J. M.; Swager, T. M., Rapid
27
28 Prototyping of Carbon-Based Chemiresistive Gas Sensors on Paper. *Proceedings of the National*
29
30 *Academy of Sciences* **2013**, *110* (35), E3265-E3270; (b) Frazier, K. M.; Mirica, K. A.; Walsh, J.
31
32 J.; Swager, T. M., Fully-drawn Carbon-based Chemical Sensors on Organic and Inorganic
33
34 Surfaces. *Lab on a Chip* **2014**, *14* (20), 4059-4066; (c) Mitchell, H. T.; Noxon, I. C.; Chaplan, C.
35
36 A.; Carlton, S. J.; Liu, C. H.; Ganaja, K. A.; Martinez, N. W.; Immoos, C. E.; Costanzo, P. J.;
37
38 Martinez, A. W., Reagent Pencils: a New Technique for Solvent-free Deposition of Reagents
39
40 onto Paper-based Microfluidic Devices. *Lab on a Chip* **2015**, *15* (10), 2213-2220.
41
42
43
44
- 45 11. Mirica, K. A.; Weis, J. G.; Schnorr, J. M.; Esser, B.; Swager, T. M., Mechanical Drawing
46
47 of Gas Sensors on Paper. *Angewandte Chemie International Edition* **2012**, *51* (43), 10740-10745.
48
49
50
- 51 12. Han, J.-W.; Kim, B.; Li, J.; Meyyappan, M., Carbon Nanotube Ink for Writing on
52
53 Cellulose Paper. *Materials Research Bulletin* **2014**, *50*, 249-253.
54
55
56
57
58
59
60

1
2
3 13. Bandothkar, A. J.; Jia, W.; Ramírez, J.; Wang, J., Biocompatible Enzymatic Roller Pens
4 for Direct Writing of Biocatalytic Materials: “Do it Yourself” Electrochemical Biosensors.
5
6 *Advanced healthcare materials* **2015**, *4* (8), 1215-1224.
7

8
9
10 14. Su, J.-J.; Beardslee, L.; Brand, O. In *Combined chemoresistive and chemocapacitive*
11 *microsensor structures*, Solid-State Sensors, Actuators and Microsystems (TRANSDUCERS &
12 EUROSENSORS XXVII), 2013 Transducers & Euroensors XXVII: The 17th International
13 Conference on, IEEE: 2013; pp 258-261.
14
15
16
17
18

19
20 15. Zhang, D.; Tong, J.; Xia, B., Humidity-sensing Properties of Chemically Reduced
21 Graphene Oxide/Polymer Nanocomposite Film Sensor Based on Layer-by-Layer Nano Self-
22 Assembly. *Sensors and Actuators B: Chemical* **2014**, *197*, 66-72.
23
24
25
26
27

28 16. Zampetti, E.; Pantalei, S.; Muzyczuk, A.; Bearzotti, A.; De Cesare, F.; Spinella, C.;
29 Macagnano, A., A high Sensitive NO₂ Gas Sensor Based on PEDOT–PSS/TiO₂ Nanofibres.
30
31 *Sensors and Actuators B: Chemical* **2013**, *176*, 390-398.
32
33
34
35

36 17. Rivadeneyra, A.; Fernández-Salmerón, J.; Agudo-Acemel, M.; López-Villanueva, J. A.;
37 Capitán-Vallvey, L. F.; Palma, A. J., Hybrid Printed Device for Simultaneous Vapors Sensing.
38
39 *IEEE Sensors Journal* **2016**, *16* (23), 8501-8508.
40
41
42
43

44 18. Ge, X.; Kostov, Y.; Rao, G., Low-Cost Noninvasive Optical CO₂ Sensing System for
45 Fermentation and Cell Culture. *Biotechnology and bioengineering* **2005**, *89* (3), 329-334.
46
47
48

49 19. (a) Young, S.-J.; Lin, Z.-D., Sensing Performance of Carbon Dioxide Gas Sensors with
50 Carbon Nanotubes on Plastic Substrate. *ECS Journal of Solid State Science and Technology*
51
52 **2017**, *6* (5), M72-M74; (b) Schütt, F.; Postica, V.; Adelung, R.; Lupan, O., Single and
53
54
55
56
57
58
59
60

1
2
3 Networked ZnO–CNT Hybrid Tetrapods for Selective Room-Temperature High-Performance
4 Ammonia Sensors. *ACS Applied Materials & Interfaces* **2017**, *9* (27), 23107-23118.

5
6
7
8
9 20. (a) Liu, S. F.; Lin, S.; Swager, T. M., An Organocobalt–Carbon Nanotube Chemiresistive
10 Carbon Monoxide Detector. *ACS sensors* **2016**, *1* (4), 354-357; (b) Jung, D.; Han, M.; Lee, G. S.,
11 Humidity-sensing Characteristics of Multi-Walled Carbon Nanotube Sheet. *Materials Letters*
12 **2014**, *122*, 281-284; (c) Jung, D.; Kim, J.; Lee, G. S., Enhanced humidity-sensing response of
13 metal oxide coated carbon nanotube. *Sensors and Actuators A: Physical* **2015**, *223*, 11-17.

14
15
16
17
18
19
20
21 21. (a) Eising, M.; Cava, C. E.; Salvatierra, R. V.; Zarbin, A. J. G.; Roman, L. S., Doping
22 Effect on Self-Assembled Films of Polyaniline and Carbon Nanotube Applied as Ammonia Gas
23 Sensor. *Sensors and Actuators B: Chemical* **2017**, *245*, 25-33; (b) Ellis, J. E.; Star, A., Carbon
24 Nanotube-based Gas Sensors toward Breath Analysis. *ChemPlusChem* **2016**.

25
26
27
28
29
30
31 22. (a) Hester, J. G.; Tentzeris, M. M.; Fang, Y. In *Inkjet-printed, flexible, high performance,*
32 *carbon nanomaterial based sensors for ammonia and DMMP gas detection*, Microwave
33 Conference (EuMC), 2015 European, IEEE: 2015; pp 857-860; (b) Hannon, A.; Lu, Y.; Li, J.;
34 Meyyappan, M., Room Temperature Carbon Nanotube Based Sensor for Carbon Monoxide
35 Detection. *Journal of Sensors and Sensor Systems* **2014**, *3* (2), 349.

36
37
38
39
40
41
42
43 23. Abdelhalim, A.; Winkler, M.; Loghin, F.; Zeiser, C.; Lugli, P.; Abdellah, A., Highly
44 Sensitive and Selective Carbon Nanotube-Based Gas Sensor Arrays Functionalized with
45 Different Metallic Nanoparticles. *Sensors and Actuators B: Chemical* **2015**, *220*, 1288-1296.

46
47
48
49
50
51 24. Contés-de Jesús, E.; Li, J.; Cabrera, C. R., Latest Advances in Modified/Functionalized
52 Carbon Nanotube-Based Gas Sensors. **2013**.

1
2
3 25. (a) Abdelhalim, A.; Falco, A.; Loghin, F.; Lugli, P.; Salmerón, J. F.; Rivadeneyra, A. In
4 *Flexible NH₃ sensor based on spray deposition and inkjet printing*, SENSORS, 2016 IEEE,
5 IEEE: 2016; pp 1-3; (b) Falco, A.; Salmerón, J.; Loghin, F.; Abdelhalim, A.; Lugli, P.;
6 Rivadeneyra, A. In *Optimization of process parameters for inkjet printing of CNT random*
7 *networks on flexible substrates*, Nanotechnology (IEEE-NANO), 2016 IEEE 16th International
8 Conference on, IEEE: 2016; pp 487-490.

9
10
11
12
13
14
15
16
17
18 26. Falco, A.; Rivadeneyra, A.; Loghin, F. C.; Salmerón, J. F.; Lugli, P.; Abdelhalim, A.,
19 Towards Low-Power Electronics: Self-Recovering and Flexible Gas Sensors. *Journal of*
20 *Materials Chemistry A* **2018**.

21
22
23
24
25
26 27. Albrecht, A.; Rivadeneyra, A.; Abdellah, A.; Lugli, P.; Salmerón, J. F., Inkjet Printing
27 And Photonic Sintering of Silver and Copper Oxide Nanoparticles for Ultra-Low-Cost
28 Conductive Patterns. *Journal of Materials Chemistry C* **2016**, *4* (16), 3546-3554.

29
30
31
32
33 28. Abdellah, A.; Abdelhalim, A.; Loghin, F.; Kohler, P.; Ahmad, Z.; Scarpa, G.; Lugli, P.,
34 Flexible carbon nanotube based gas sensors fabricated by large-scale spray deposition. *Sensors*
35 *Journal, IEEE* **2013**, *13* (10), 4014-4021.

36
37
38
39
40
41 29. Colasanti, S.; Robbiano, V.; Loghin, F. C.; Abdelhalim, A.; Bhatt, V. D.; Abdellah, A.;
42 Cacialli, F.; Lugli, P., Experimental and Computational Study on the Temperature Behavior of
43 CNT Networks. *IEEE Transactions on Nanotechnology* **2016**, *15* (2), 171-178.

44
45
46
47
48
49 30. Lin, Z.-D.; Young, S.-J.; Chang, S.-J., Carbon Nanotube Thin Films Functionalized Via
50 Loading of Au Nanoclusters for Flexible Gas Sensors Devices. *IEEE Transactions on Electron*
51 *Devices* **2016**, *63* (1), 476-480.

1
2
3 31. (a) Penza, M.; Rossi, R.; Alvisi, M.; Signore, M.; Cassano, G.; Dimaio, D.; Pentassuglia,
4 R.; Piscopiello, E.; Serra, E.; Falconieri, M., Characterization of Metal-Modified and Vertically-
5 Aligned Carbon Nanotube Films for Functionally Enhanced Gas Sensor Applications. *Thin Solid*
6 *Films* **2009**, *517* (22), 6211-6216; (b) Star, A.; Joshi, V.; Skarupo, S.; Thomas, D.; Gabriel, J.-C.
7 P., Gas Sensor Array Based on Metal-Decorated Carbon Nanotubes. *The Journal of Physical*
8 *Chemistry B* **2006**, *110* (42), 21014-21020.

9
10
11
12
13
14
15
16
17
18 32. Zhang, D.; Wang, K.; Tong, J.; Xia, B., Characterization of Layer-by-Layer Nano Self-
19 Assembled Carbon Nanotube/Polymer Film Sensor for Ethanol Gas Sensing Properties.
20 *Microsystem technologies* **2014**, *20* (3), 379-385.

21
22
23
24
25
26 33. Zhao, H.; Zhang, T.; Qi, R.; Dai, J.; Liu, S.; Fei, T., Drawn on Paper: A Reproducible
27 Humidity Sensitive Device by Handwriting. *ACS applied materials & interfaces* **2017**, *9* (33),
28 28002-28009.

29
30
31
32
33 34. Honda, W.; Harada, S.; Arie, T.; Akita, S.; Takei, K. In *Printed wearable temperature*
34 *sensor for health monitoring*, IEEE SENSORS 2014 Proceedings, IEEE: 2014; pp 2227-2229.

1
2
3 **Realization of resistive CNT-based gas sensor on flexible substrate with a ball pen,**
4 **exhibiting performance comparable to higher cost technologies.** For its fabrication, both
5 commercial and custom-made inks are employed, broadening the use of this technology. Such
6 a solution provides a fast prototyping tool and opens the electronics – and the sensors world -
7 to the so-called do-it-yourself (DIY) paradigm
8

9 **Ball pen, carbon nanotubes, flexible substrate, resistive sensor, silver nanoparticles**

11 F. C. Loghin*, A. Falco, A. Albrecht, J. F. Salmerón, M. Becherer, P. Lugli, A.
12 Rivandeneira*

14 **A handwriting method for low-cost gas sensors**

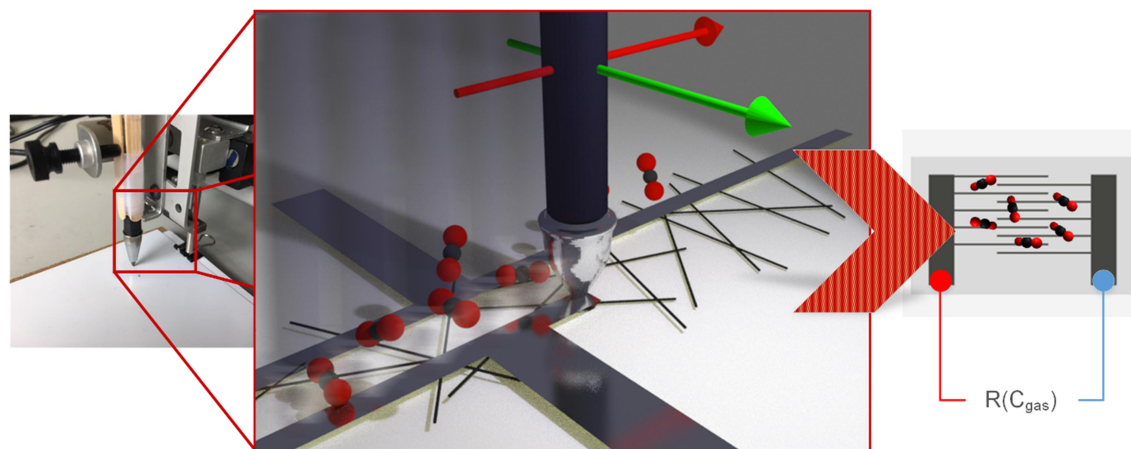




Figure 1. (a) Photograph of ball pen in the robot arm employed to develop the printed sensor
338x254mm (96 x 96 DPI)



Figure 2. (a) Photograph of the fabricated sensor;

254x338mm (96 x 96 DPI)

1
2
3
4
5
6
7
8
9
10
11
12
13
14
15
16
17
18
19
20
21
22
23
24
25
26
27
28
29
30
31
32
33
34
35
36
37
38
39
40
41
42
43
44
45
46
47
48
49
50
51
52
53
54
55
56
57
58
59
60

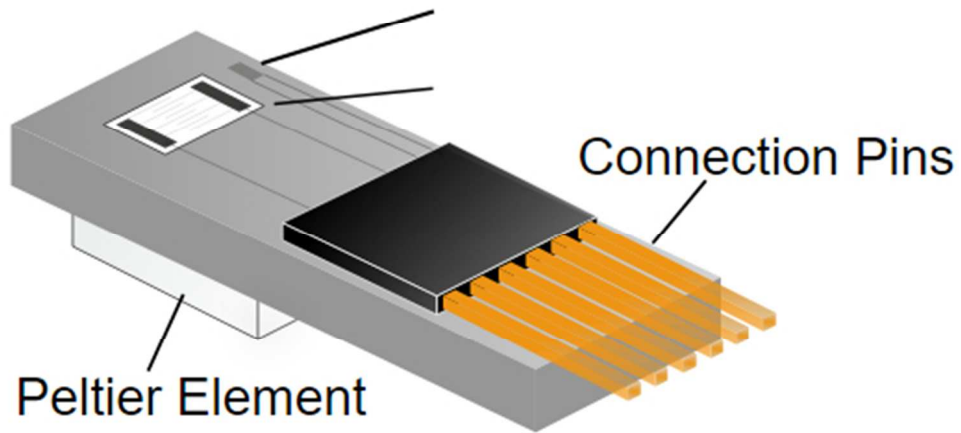


Figure 2. (b) schematic depicting the sensor module

143x75mm (96 x 96 DPI)

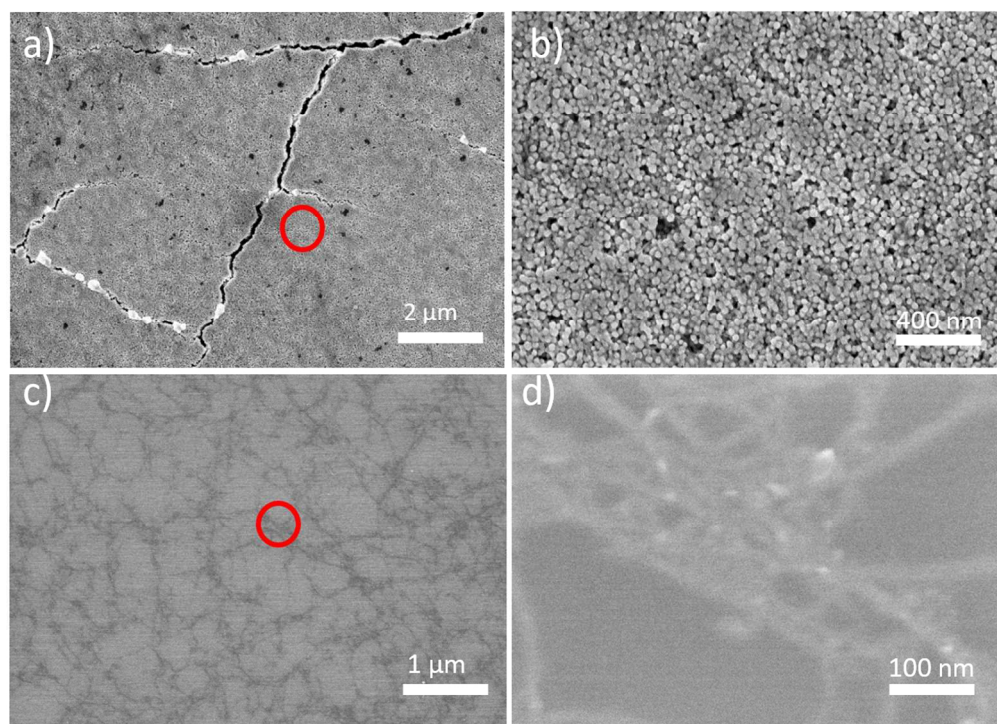


Figure 3. (a-b) Scanning electron microscope image of the silver nanoparticle film at (a) 5K (1 μm scale) and (b) 25 K (200 nm scale bar) magnification with the red circle depicting the higher magnification region. (c-d) Scanning electron microscope image of the CNT film at (a) 20K (1 μm scale) and (b) 200K (100 nm scale bar) magnification with the red circle depicting the higher magnification region.

364x263mm (96 x 96 DPI)

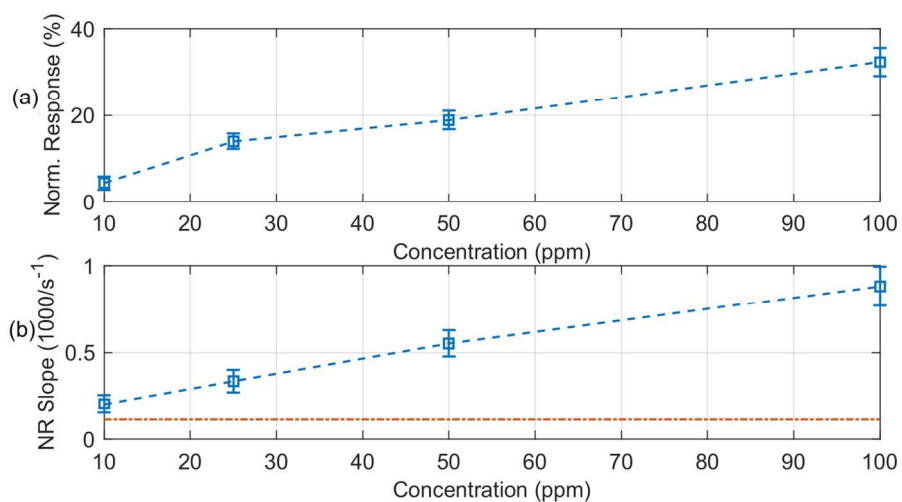


Figure 4. Response to NH_3 (a) Normalized resistance vs. concentration; (b) Average slope of the normalized response in the first 150 s of exposure. The red dashed line indicates the average slope of the normalized response in the last 150 s of cooling time.

499x255mm (96 x 96 DPI)

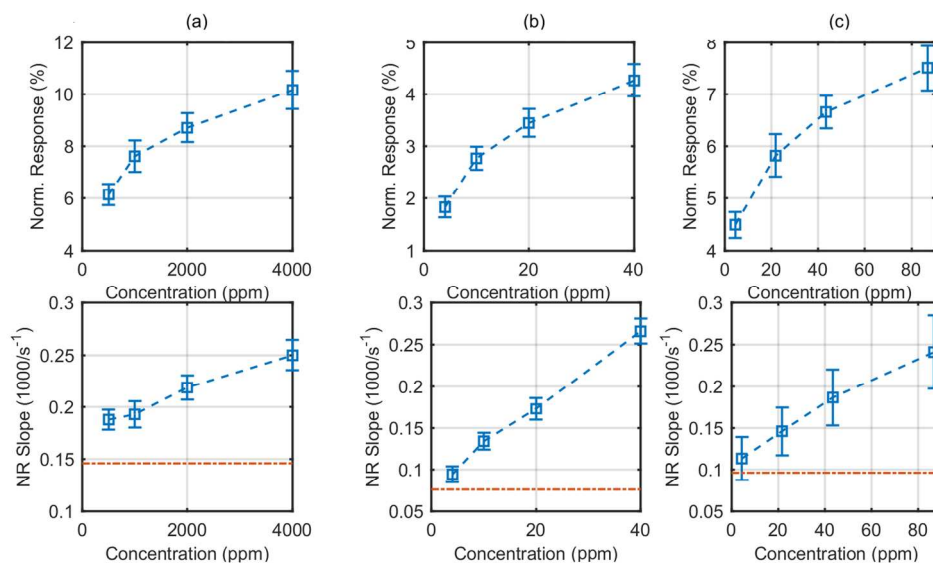


Figure 5. First row corresponds to the normalized resistance, bottom row to average slope of the normalized response in the first 150 s of exposure vs. concentration for (a) CO₂, (b) CO and (c) Ethanol. In the bottom row the red dashed line indicates the average slope of the normalized response in the last 150 s of cooling time.

499x288mm (96 x 96 DPI)

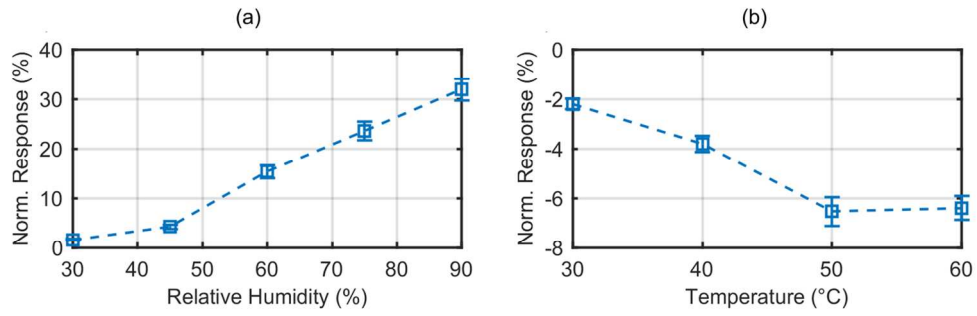


Figure 6. Normalized resistance vs. concentration for (a) RH and (b) Temperature.

430x139mm (96 x 96 DPI)

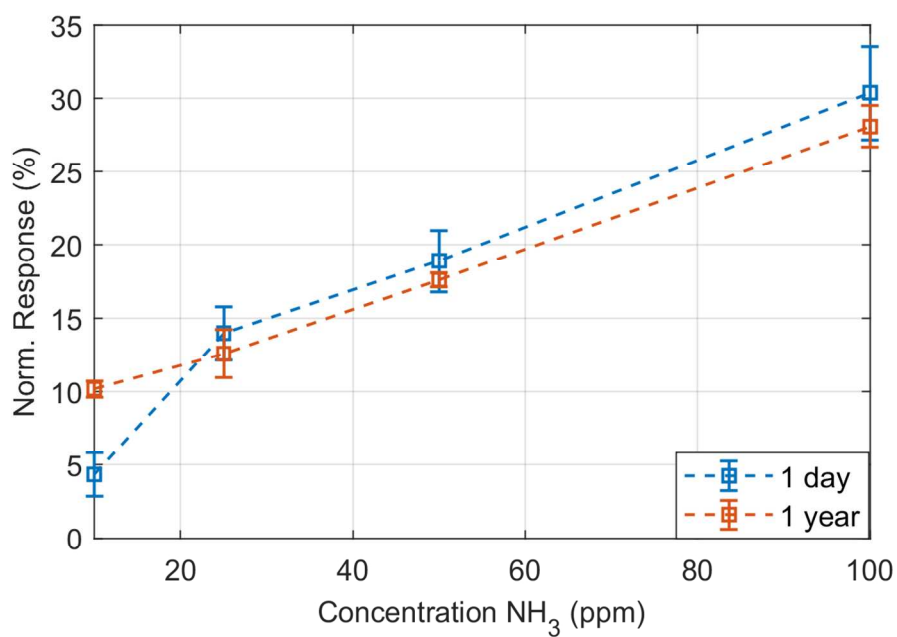


Figure 7. Normalized response with respect to different concentrations of NH₃ for the same sensor one day after fabrication (blue line) and one year after fabrication (orange line).

119x80mm (300 x 300 DPI)